*Structural Engineering and Mechanics, Vol. 28, No. 3 (2008) 335-351*
DOI: http://dx.doi.org/10.12989/sem.2008.28.3.335


# Design on a new oil well test shock absorber under impact load*

Yuanxun Wang† and Peng Zhang‡

*Huazhong University of Science and Technology, Wuhan, 430074, P.R. China*

Zhijian Cui‡†

*Huazhong University of Science and Technology, Wuhan, 430074, P.R. China*
*Xi'an Shiyou University, Xi'an, 710065, P.R. China*

Chuanyao Chen‡‡

*Huazhong University of Science and Technology, Wuhan, 430074, P.R. China*

*(Received September 12, 2006, Accepted November 16, 2007)*

**Abstract.** Continuous operation of test and measurement is a new operating technique in the petroleum exploitation, which combines perforation with test and measurement effectively. In order to measure the original pressure of stratum layer exactly and prevent testing instrument from being impaired or damaged, a suitable shock absorber is urgently necessary to research. Based on the attempt on the FEM analysis and experiment research, a new shock absorber is designed and discussed in this paper. 3D finite element model is established and simulated accurately by LS-DYNA, the effect and the dynamic character of the shock absorber impact by half sinusoidal pulse force under the main lobe frequency are discussed both on theoretics and experiment. It is shown that the new designed shock absorber system has good capability of shock absorption for the impact load.

**Keywords:** shock absorber; disturbing force; groundsill; absorption coefficient; impact strength; main lobe frequency.

## 1. Introduction

Petroleum well test is an important and difficult engineering for the oil exploitation. Continuous operation of test and measurement is a new operating technique in the petroleum production, which combines perforation with test and measurement effectively. In the process of the test operation, the perforation gun, detonating set, shock absorber, press difference set, secluding set, pressure meter or

† Associate Professor, Corresponding author, E-mail: wooshin@163.com
‡ Graduate Student, E-mail: zhangpeng01061014@163.com
‡† Associate Professor, Corresponding author, E-mail: zhjcui@xsyu.edu.cn
‡‡ Professor, E-mail: chency00@mail.hust.edu.cn
*Project supported by the Xinjiang Petroleum Management Bureau of China

other stratum test apparatus are connected in series as a test tubular column which is called as the oil well test pipe. When the perforation gun under the bottom of the well shoots cannonballs for the oil route-way holes, it will bring huge impact shock with pressure about 30~100 MPa according the theory calculation and practical test (Velichkovich 2005). In order to measure the original pressure of stratum layer exactly and prevent testing instrument from being impaired or damaged, it is urgently necessary to research a suitable shock absorber.

The conventional shock absorbers for the oil well test adopted some low stiffness and high damping plastic rings as the spring element of the shock absorber to make the oil well test system absorb and isolate from shake energy produced by the perforation gun shoot under the bottom of the oil well. For the stiffness of the spring element is small, shock absorption is principally acted by separating from the shake. If the stiffness of the spring element is very small, such as charge inner tube of a car or large cotton mat, the shock absorption is better. But the stiffness of the spring element could not be very small for the cubage limited of the oil well, the shock absorption effect is limited.

It is very important to understand the dynamic characters of the system under impact load for the research of the well test shock absorber system. But it is very difficult to describe theoretically for a complex oil well in which fill in high press slurry and oil coupled interactions exist in perforation gun shoot behaviors. Up to now, the correlative report is rarely found on it. Over the years, the only way for the shock absorber research is mainly through a trial-and-error approach, but optimization by trial-and-error can be very expensive and time consuming. Recently, numerical method provides a powerful tool in studying these interactions and complex process. One of the most important developments was the introduction of the dynamic explicit finite-element method (FEM) which has the advantage of less memory requirement and higher computational efficiency, and can deal with nonlinear behaviors and complex boundary conditions (Fortgang and Singhose 2002, He *et al.* 2000, Choi and Hong 2004, Johan *et al.* 2004, Gao *et al.* 2004). Based on the attempt on the FEM analysis and experiment research, a new designed shock absorber with good capability of shock absorption for the impact load is discussed in this paper.

## 2. Design of the shock absorber

### *2.1 Structure of the new shock absorber*

In the process of the oil well test operation, the oil well test pipe with the length about 4000 to 6000 m is constitute with the perforation gun, detonating set, shock absorber, press difference set, secluding set, pressure meter or other stratum test apparatus, see Fig. 1. The shock absorber must be set between the perforation gun and the oil well test pipe to keep the test device from being damaged. The secluding set keeps the inner of the oil pipe separate from the out of the oil well, and make the slurry in the well separate from the oil. Also it can restrain the transverse and torsional vibration to transmit to the up testing instruments.

To reduce the huge impact energy in the limited space and prevent testing instrument from being impaired or damaged, the structure of the new designed shock absorber system is show as Fig. 2. Four low stiffness and high damping plastic rings and three high stiffness springs alternated in series are adopted as the spring element of the shock absorber system. By the alternately acting of spring absorbing and plastic isolating from shake, make the system absorb and separate from shake

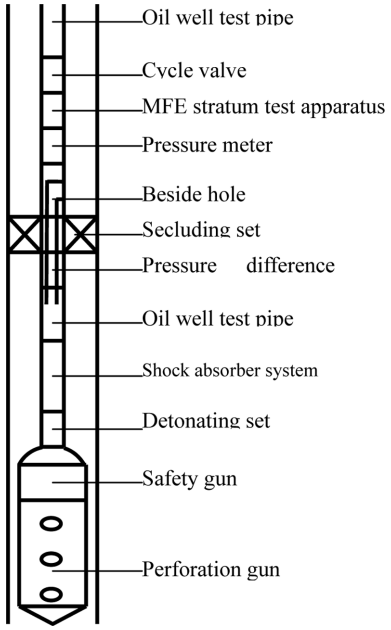


Fig. 1 Oil well test pipe structure schematic

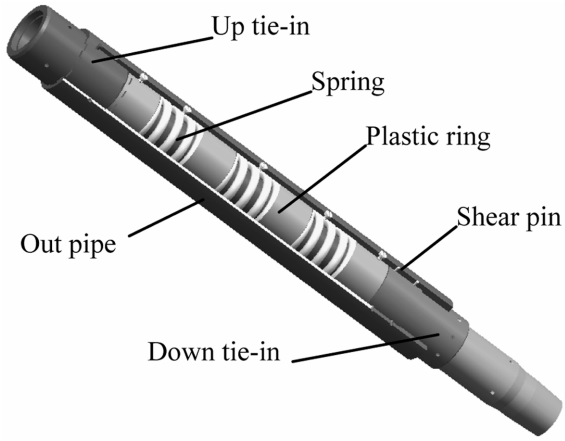


Fig. 2 The structure of the new shock absorber system

energy produced by the perforation gun shoot under the bottom of the oil well and the lognitudinal vibration of the oil well test pipe. The up tie-in connects with the oil well test pipe and the down tie-in connects with the perforation gun detonating set. The out pipe separates the inner oil with the outer slurry in the well. Also there is some shear pins connect the out pipe with the down tie-in and high viscidity oil fill in the cavum between the out pipe and the inner pipe. When the huge impact energy act on the shock absorber, the shear pins will be broken and absorb the impact energy first. The high viscidity oil is good for shock absorption but is difficult for analysis.

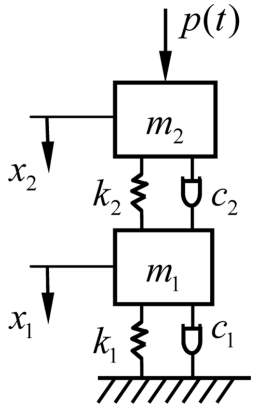


Fig. 3 Vibration model of the shock absorber system

### 2.2 Analysis of the theory of shock absorber system

The shock absorber is set between the perforation gun under the bottom of the well and the oil well test pipe. The secluding set between the oil pipe can restrict its transverse and torsional vibration. The slurry in the well and the high viscidity oil fill in the shock absorber are very difficult to describe theoretically. But the damping of the slurry and the oil is good for reducing amplitude and changing the phase of the vibration. So it's favorable for the design of the shock absorber to ignore the damping of the slurry and the high viscidity oil. Make the oil well test pipe and the perforation gun as a concentrated mass $m_1$ and $m_2$, the shock absorber system can be simplified as a two mass and two freedom vibration system (Hartog 1985), see Fig. 3.

For the shock absorber system, $m_1$ is the oil well test pipe mass, $m_2$ is the perforation gun mass, $k_1$ and $c_1$ is the stiffness and damping of the ground base, $k_2$ and $c_2$ is the stiffness and damping of the shock absorber system, $p(t)$ is the impact shock force, with very short duration and acts as a pulse signal to the shock absorber system. The total impulse is

$$I = \int_0^\tau p(t)dt \tag{1}$$

As duration of the shock force $\tau$ is much lesser than the cycle of the shock absorber system, the velocity of $m_1$ after shock can be given as

$$\dot{u}_m = \frac{I}{m_2} \tag{2}$$

The differential equation of the vibration model of the shock absorber system is given by He *et al.* (2000)

$$m_1\ddot{x}_1 + (c_1 + c_2)\dot{x}_1 + (k_1 + k_2)x_1 = c_2\dot{x}_2 + k_2x_2 \tag{3}$$

$$m_2\ddot{x}_2 + c_2\dot{x}_2 + k_2x_2 = c_2\dot{x}_1 + k_2x_1 \tag{4}$$

From Eqs. (3) and (4), the differential equation can be written as

$$\ddot{\mathbf{x}}_1 + 2\zeta_1\omega_1\dot{\mathbf{x}}_1 + \omega_1^2\mathbf{x}_1 = -\mu\ddot{\mathbf{x}}_2 \tag{5}$$

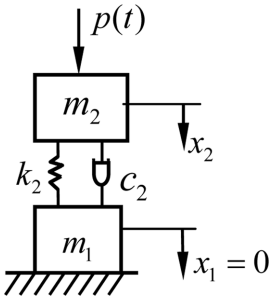


Fig. 4 Vibration model of the shock absorber system with $x_1 = 0$

where

$$\mu = \frac{m_2}{m_1}, \quad \omega_1 = \left(\frac{k_1}{m_1}\right)^{1/2}, \quad \zeta_1 = \frac{c_1}{2(m_1 k_1)^{1/2}} \tag{6}$$

The system is static before shock, the initial condition is

$$x_1(0) = \ddot{x}_1(0) = 0 \tag{7}$$

For $m_2 << m_1$, $k_1$ and $c_1$ is much bigger, $x_1$ is much lesser than $x_2$, the effect of $x_1$ to $x_2$ can be ignored. Thus, the vibration model of the shock absorber system can be simplified as Fig. 4 with $x_1 = 0$.

With $x_1 = 0$, make the relatively $\delta_1 = x_1$ and $\delta_2 = x_2$ as the generalized coordinates, the differential equation of the vibration model of the shock absorber system is given by

$$\ddot{\delta}_2 + 2\zeta_2\omega_2\dot{\delta}_2 + \omega_2^2\delta_2 = 0 \tag{8}$$

where

$$\omega_2 = \left(\frac{k_2}{m_2}\right)^{1/2}, \quad \zeta_2 = \frac{c_2}{2(m_2 k_2)^{1/2}} \tag{9}$$

Make the shock end point position $\delta_1$ of the oil well test pipe mass $m_1$ as the coordinate origin, and the time as the time coordinate origin, the initial condition is

$$\delta_2(0) = 0, \quad \dot{\delta}_2(0) = \dot{u}_m \tag{10}$$

According the initial condition (10), the analytic resolution of relatively displacement $\delta_2$ of the pipe can be given by Eq. (8). For $x_1 = 0$, $\delta_2 = x_2$, the analytic resolution of $\ddot{x}_2$ can be given by differential $\delta_2$. Then according the initial condition (7), the analytic resolution of $x_1$ can be given by Eq. (5). The disturbance power $N$ brought by the impact force $p(t)$ can be obtained from the following equation

$$N = c_1\dot{x}_1 + k_1 x_1 \tag{11}$$

For vibration model of the shock absorber system, see Fig. 3, ignore the damping of the system,

make the relatively $\delta_1 = x_1$ and $\delta_2 = x_2 - x_1$ as the generalized coordinates, the differential equation of the shock absorber system is given by Hartog (1985)

$$\begin{aligned} \ddot{\delta}_2 + \omega_2^2 \delta_2 &= -\ddot{\delta}_1 \\ \ddot{\delta}_1 + \omega_1^2 \delta_1 &= \mu \omega_2^2 \delta_2 \end{aligned} \tag{12}$$

the initial condition is

$$\delta_1(0) = \dot{\delta}_1(0) = \delta_2(0) = 0, \quad \dot{\delta}_2(0) = \dot{u}_m \tag{13}$$

According the initial condition (13), the analytic resolution of relatively displacement $\delta_1$ and $\delta_2$ of the oil well test pipe can be given by Eq. (12). For $x_1 = \delta_1$, from Eq. (11), the disturbance power $N$ can be obtained.

The maximum distortion of the secondary stage spring $\delta_{2m}$ and the maximum disturbance power $N_m$ is

$$\delta_{2m} = \frac{I}{m_2 \omega_2} \left[ 1 + \frac{\mu}{(1+f_1)^2} \right]^{-1/2} \tag{14}$$

$$N_m = \frac{I}{m_2 \omega_2} [(1-f_1)^2 + \mu]^{-1/2} \tag{15}$$

where

$$\mu = \frac{m_2}{m_1}, \quad f_1 = \frac{\omega_1}{\omega_2} \tag{16}$$

The maximum impact force is $p_m$, the shock absorption coefficient $n$ is

$$n = \frac{N_m}{p_m} = \frac{I}{p_m m_2 \omega_2} [(1-f_1)^2 + \mu]^{-1/2} \tag{17}$$

From Eqs. (15) and (16), the relationship of $\delta_{2m}$, $N_m$ and the natural frequency ratio $f_1$ can be shown as Fig. 5 and Fig. 6 and obtained follow conclusions.

a. Increasing $m_1$ and $k_1$, the natural frequency $\omega_1$ and $\omega_2$ are almost invariable, and the maximum disturbance power $N_m$ and the maximum distortion of the secondary stage spring $\delta_{2m}$ are changeless too.
b. Increasing $m_2$ and $k_2$, the natural frequency ratio $f_1$ is invariable, the maximum disturbance power $N_m$ is changeless, the maximum distortion of the secondary stage spring $\delta_{2m}$ is increased pro rata with $(m_2 k_2)^{1/2}$.
c. When the natural frequency ratio $f_1$ is close to 1, the maximum disturbance power $N_m$ is close to the maximum. Make the natural frequency ratio $f_1$ much bigger than 1, the maximum disturbance power $N_m$ will be reduced evidently.
d. Increasing mass $m_1$, reducing stiffness $k_1$, the natural frequency $\omega_1$ would be reduced. Keep the secondly stage parameter reduce, the natural frequency ratio $f_1$ is reduced, the maximum disturbance power $N_m$ is reduced evidently, and even $f_1$ is close to 1, the maximum disturbance power $N_m$ would be reduced.

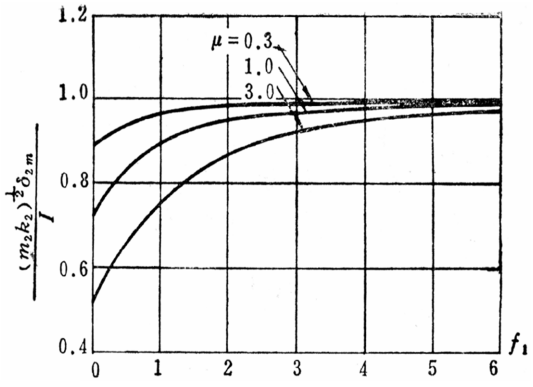


Fig. 5 The relationship curve of mass ratio $\mu$, $\delta_m$ and natural frequency ratio

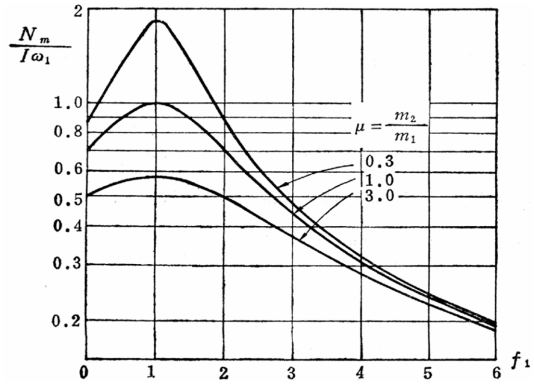


Fig. 6 The relationship curve of mass ratio $\mu$, $N_m/I\omega_1$ and natural frequency ratio

## 3. FEM model and analysis

### *3.1 FEM model of the shock absorber system*

For the shock absorber system, the effect factors are complex, the parametric analysis is used to take the effect factors as variables with the APDL (analysis parametric design language) of ANSYS. The impact power acting on the shock absorber system transfers from the bottom to the upper. Closing to the working state, simplify the bottom of the shock absorber as a cylinder and the upper as a square part, take the three springs as 48 lines for each spring to reduce the stress concentration, the FEM model of the shock absorber system is shown as Fig. 7. The model was meshed using Esize and relational command to control the elements.

### *3.2 Governing equations*

The moving equation of the shock absorber system, based on the sandglass stickiness damping

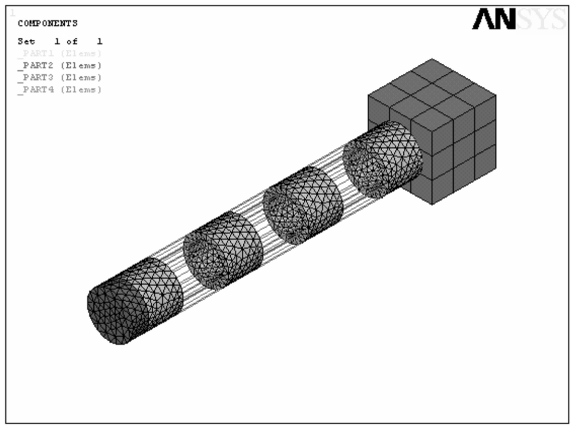


Fig. 7 FEM model of the shock absorber system

control, can be written as (Johan *et al.* 2004, Gao *et al.* 2004, Kim *et al.* 2002, Hartog 1985, Pennestri 1998)

$$M\ddot{x}(t) + F(x, \dot{x}) - P(x, t) = H \tag{18}$$

where, $M$ is the general mass matrix, $\ddot{x}(t)$ is the general node acceleration vector matrix, $F$ is the equivalent node force vector matrix of the cell stress field, $P$ is the general node vector matrix, and $H$ is the general sandglass stickiness damping force fit together by the cell node sandglass stickiness damping force. Considering the damping $c$, Eq. (18) can be written as

$$M\ddot{x}(t) + c\dot{x} + F(x, \dot{x}) - P(x, t) = H \tag{19}$$

the time integral using explicit center difference method can be written as

$$\begin{aligned} \ddot{x}(t_n) &= M^{-1}[P(t_n) + H(t_n) - c\dot{x}(t_{n-\frac{1}{2}})] \\ \dot{x}\left(t_{n+\frac{1}{2}}\right) &= \dot{x}\left(t_{n-\frac{1}{2}}\right) + \frac{1}{2}(\Delta t_{n-1} + \Delta t_n)\ddot{x}(t_n) \\ x(t_{n+1}) &= x(t_n) + \Delta t_n \dot{x}\left(t_{n+\frac{1}{2}}\right) \end{aligned} \tag{20}$$

where, $t_{n-\frac{1}{2}} = \frac{1}{2}(t_n + t_{n-1})$, $t_{n+\frac{1}{2}} = \frac{1}{2}(t_{n+1} + t_n)$, $\Delta t_{n-1} = (t_n - t_{n-1})$, $\Delta t_n = (t_{n+1} - t_n)$, $\ddot{x}(t_n)$, $\dot{x}\left(t_{n+\frac{1}{2}}\right)$, $x(t_{n+1})$ is the node acceleration vector at $t_n$, the node speed vector at $t_{n+\frac{1}{2}}$, and the node coordinate vector at $t_{n+1}$.

For the centralized mass matrix $M$, the solution of Eq. (20) is non-coupling, but it needs control condition for the stability of the explicit center difference method (Gao *et al.* 2004). The LS-DYNA program uses time change step increment method to get the time step by the currently stability control condition (Pennestri 1998, Song *et al.* 2005, John *et al.* 1998). At first, calculate the limit time step $\Delta t_{ci}$ of each cell $(i = 1, 2, \ldots, m)$, it is the maximum allowable time step for the stability of the explicit center difference method, then take its minimum as the next time step, that is

$$\Delta t = \min(\Delta t_{c1}, \Delta t_{c2}, \ldots, \Delta t_{cm}) \tag{21}$$

where, $\Delta t_{ci}$ is the limit time step of cell, $m$ is the cell number, and different cell type has different limit time step $\Delta t_c$, for example, for the rods cell and beam cell (John *et al.* 1998, The DYNAFORM Team 2004)

$$\Delta t_c = \alpha\left(\frac{L}{c}\right) \tag{22}$$

where, $\alpha$ is the time step factor, it's 0.9 when default. $L$ is the length of rods cell or beam cell, $c$ is the material velocity of sound, $c = \sqrt{E/\rho}$, $E$ is the elastic modulus, $\rho$ is the mass density.

For the 3D solid cell (John *et al.* 1998, The DYNAFORM Team 2004)

$$\Delta t_c = \frac{\alpha L_e}{[Q + (Q^2 + c^2)^{1/2}]} \tag{23}$$

where, $Q$ is the accessorial impact viscosity, if the particle velocity is $u$, then

$$\mathbf{Q} = \begin{cases} \mathbf{c}_1 c + \mathbf{c}_0 \mathbf{L}_e |\dot{\mathbf{u}}| & \text{for} \quad \dot{\mathbf{u}} < 0 \\ 0 & \text{for} \quad \dot{\mathbf{u}} > 0 \end{cases} \tag{24}$$

$\mathbf{L}_e$ is the character length, $\mathbf{L}_e$ is the minimum height for 4 nodes solid cell, or $\mathbf{L}_e = \mathbf{V}_e / \mathbf{A}_{e\max}$ for 8 nodes solid cell, $\mathbf{c}_1$ and $\mathbf{c}_0$ is the non dimension constants, it is 1.5 and 0.06 when default, $c$ is the material velocity of sound, $c = \sqrt{E(1-\mu)/(1+\mu)(1-2\mu)\rho}$, $E$ is the elastic modulus, $\nu$ is the Poisson ratio, $\rho$ is the mass density. $\mathbf{V}_e$ is the cell volume, $\mathbf{A}_{e\max}$ is the cell maximum side area.

The constitutive equations of the ultra-elasticity plastic material can be written as (Vegter *et al.* 2003, Yin *et al.* 2002, Kevin 2004)

$$S_{ij} = \frac{\partial W}{\partial E_{ij}} = 2\frac{\partial W}{\partial C_{ij}} \tag{25}$$

where, $S_{ij}$ is the second type of Piola-Kirchhoff stress tensor, $W$ is the strain-energy density, $E_{ij}$ is Lagrangian strain tensor, $C_{ij}$ is Cauchy-Green distortion tensor. The relationship of $E_{ij}$ and $C_{ij}$ can be written as

$$E_{ij} = \frac{1}{2}(C_{ij} - \delta_{ij}) \tag{26}$$

where, $\delta_{ij}$ is the identity matrix variable, $C_{ij}$ can be written as

$$[C] = [F]^T [F] \tag{26}$$

where, $[F] = \partial x / \partial X$, $X_i$ is the position of the material at $i$ orientation as non-distortion, $x_i$ is the position of the material at $i$ orientation after distorting.

### 3.3 Boundary conditions

Difference from the implicit formula of ANSYS, LS-DYNA differentiates the boundary as zero restriction and non-zero restriction (Song *et al.* 2005, John 1998, The DYNAFORM Team 2004). All the non-zero restrictions are taken order with load. The boundary conditions of the shock absorber system are shown as Table 1, where, *Ux*, *Uy* and *Uz* are the line displacements along *x*, *y* and *z* coordinates separately, *Rx*, *Ry* and *Rz* are the rotation displacements around *x*, *y* and *z* coordinates separately, and 0 is delegated for forbidding load and 1 for permitting.

Table 1 The boundary conditions of the new shock absorber system

| | *Ux* | *Uy* | *Uz* | *Rx* | *Ry* | *Rz* |
|---|---|---|---|---|---|---|
| Up tie-in | 0 | 0 | 0 | 0 | 0 | 0 |
| Down tie-in | 0 | 0 | 1 | 0 | 0 | 0 |
| Spring | 0 | 0 | 1 | 0 | 0 | 0 |
| Outer pipe | 0 | 0 | 0 | 0 | 0 | 0 |

The impact load acting on the shock absorber system can be equated as a half sine impulse wave. Usually the half sine impulse wave can be converted into unilateral spectrum contained only plus frequency, its amplitude is the double of the half sine impulse wave. The main lobe frequency of linearity spectrum by Fourier transform is about $3/(2\tau)$ (Choi and Hong 2004, Johan *et al.* 2004). The peak value according the definition of impact strength is

$$I = \int_0^\tau F(t)dt = \int_0^\tau F\sin\frac{\pi t}{\tau}dt = \frac{2F\tau}{\pi} = \frac{200}{\pi} \tag{28}$$

Taking the first, second and fourth phase of the Fourier transform approach the half sine impulse wave, the frequency range are 0~150 Hz, 0~750 Hz, 0~1800 Hz, and corresponding pulse time are 0.01s, (7/1500)s, (1/400)s. The pulse amplitude, with the pulse impact strength $I = 200/\pi$ N·s, are 10000N, (150000/7)N, 40000N corresponding the three frequency range respectively.

Fig. 8 and Fig. 9 show the simulating course of the disturbing force ($r2$) of the groundsill and the displacement ($d$) of the down tie-in with the frequency range is 0~750 Hz.

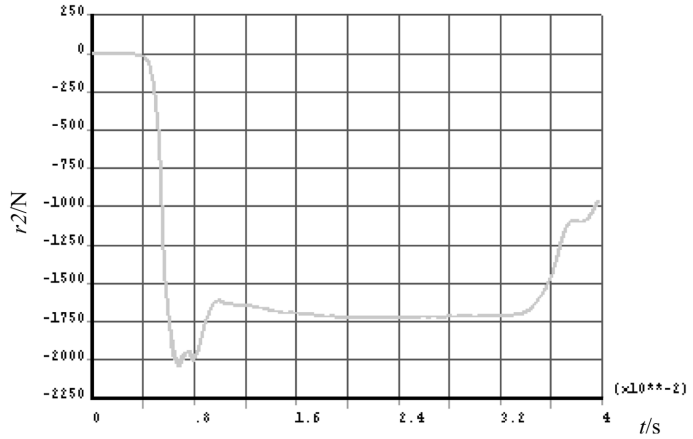


Fig. 8 The disturbing force ($r2$) course with the frequency range 0~750 Hz

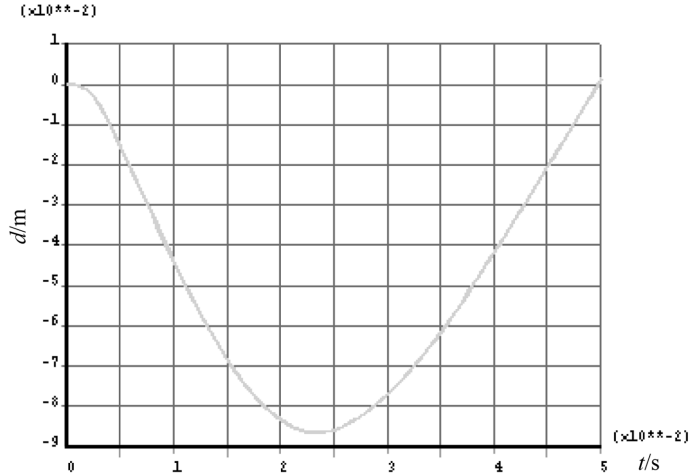


Fig. 9 The displacement ($d$) course with the frequency range 0~750 Hz

## 4. Experiment

Using dynamic disturbing test method, see Fig. 10, the dynamic characteristic of the shock absorber can be test. Disturbing the down tie-in of the shock absorber using the instantaneous disturbance with different frequency according the FEM simulating, the responses by four output channel of the test are shown as Fig. 11 to Fig. 13, where Ch1 is the input disturbing force pulse signal which is reverse in sign with the FEM simulating impact force, Ch2 to Ch5 are the response signals collected by four acceleration sensors. According the output responses and the input signal data, the shock absorption coefficient $n$ of the shock absorber can be calculated as Table 2.

Table 2 shows that the result of FEM simulating and test is coinciding well. For the simplifying of the model, the plastic material parameter given by experience, ideal impact load of the half sine impulse wave, and test error, the FEM model given in this paper is exact.

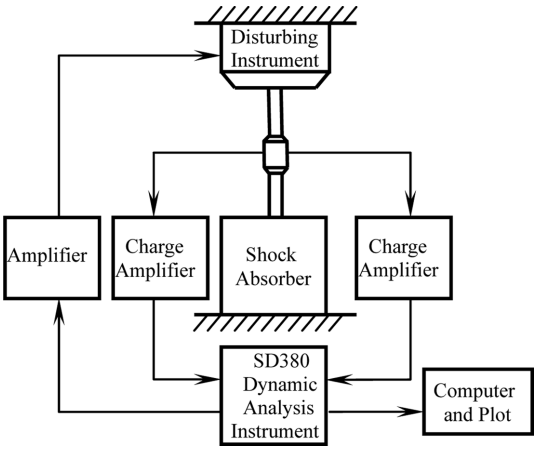


Fig. 10 Dynamic test equipment of the shock absorber

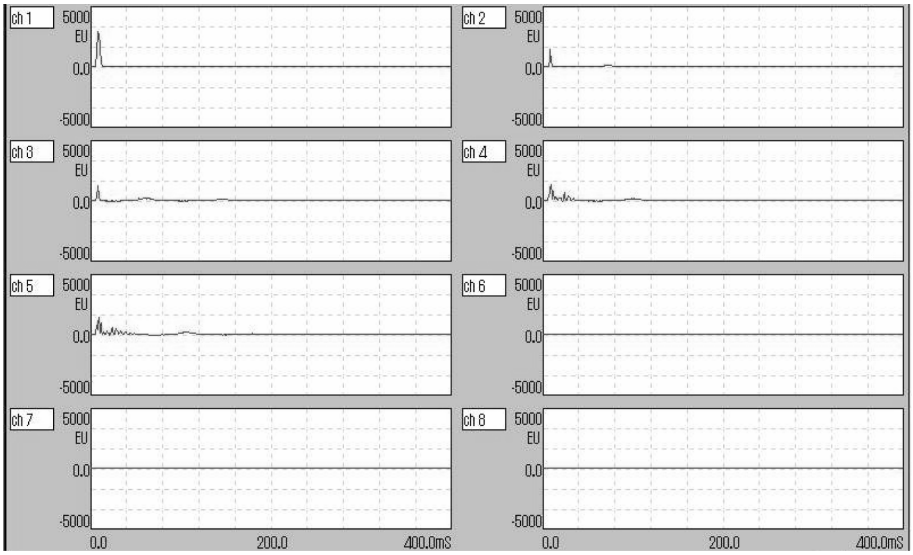


Fig. 11 Dynamic response of the shock absorber with disturbing frequency 150 Hz

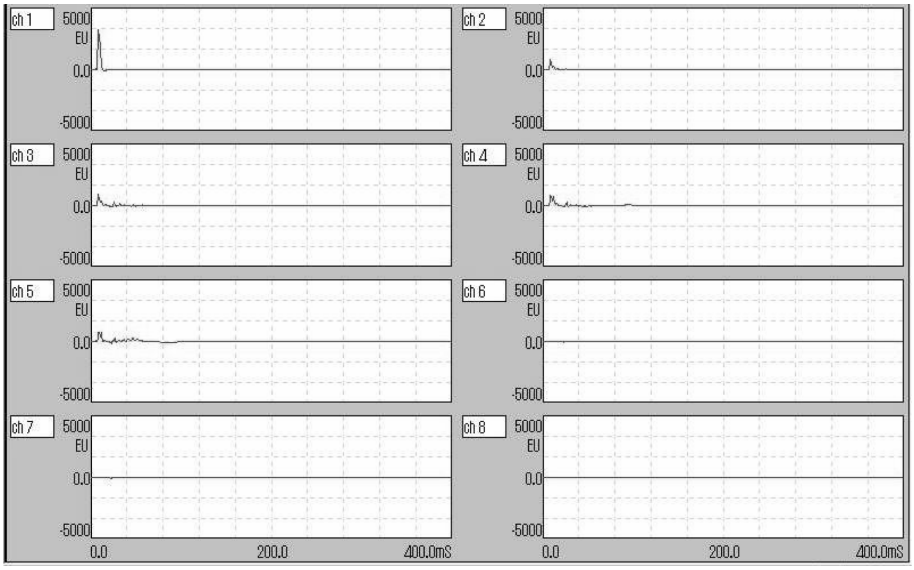


Fig. 12 Dynamic response of the shock absorber with disturbing frequency 750 Hz

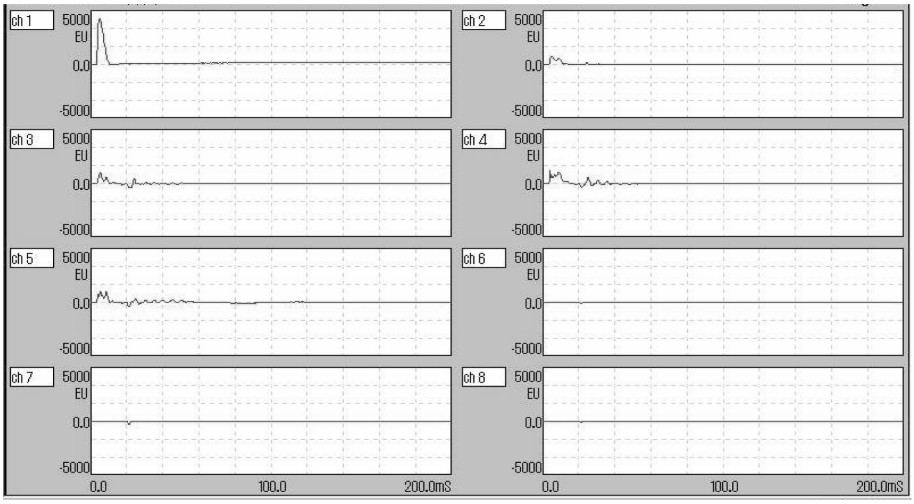


Fig. 13 Dynamic response of the shock absorber with disturbing frequency 1800 Hz

Table 2 Comparison of Coefficient ($n$) by Simulating and Test

| Frequency (Hz) | Pulse time (ms) | Pulse amplitude (N) | Max. ($r$2) (N) | Shock absorption doefficient ($n$) by simulating | Shock absorption doefficient ($n$) by test |
|---|---|---|---|---|---|
| 0~150 | 10 | 10000 | 1663 | 0.1663 | 0.1687 |
| 0~750 | 4.6667 | 21429 | 2039 | 0.0952 | 0.1061 |
| 0~1800 | 2.5 | 40000 | 3459 | 0.0865 | 0.0829 |

## 5. Simulating results and discussion

The spring stiffness, plastic material and the mass of the down tie-in are important for the design of the shock absorber system. At a certain impact strength with its main frequency 150 Hz, the disturbing force ($r2$) of the groundsill, plastic touching force ($r1$) with the down tie-in, plastic friction ($r3$) with the outer pipe and the displacement ($d$) of the down tie-in have been simulated by using LS-DYNA with different parameters and working conditions.

### *5.1 Simulating of the spring stiffness of the shock absorber system*

Fig. 14 and Fig. 15 show the simulating course of the disturbing force ($r2$) of the groundsill and the displacement ($d$) of the down tie-in with the spring stiffness $K1$ = 160000 N/m, and Table 6 shows the simulating shock absorb coefficient $n$ and the extremum of the disturbing force ($r2$) of

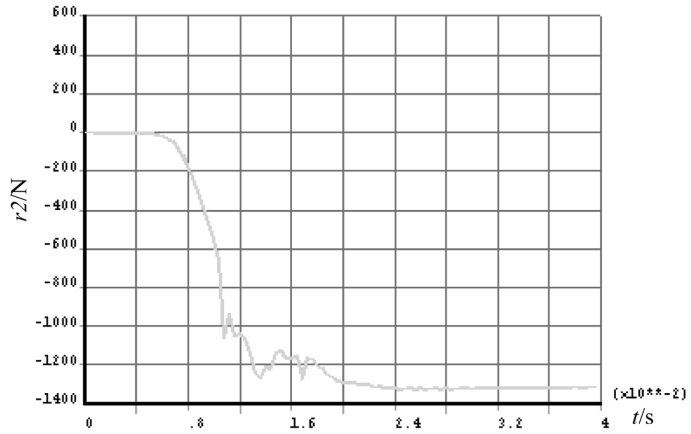


Fig. 14 The disturbing force ($r2$) course with $K1$

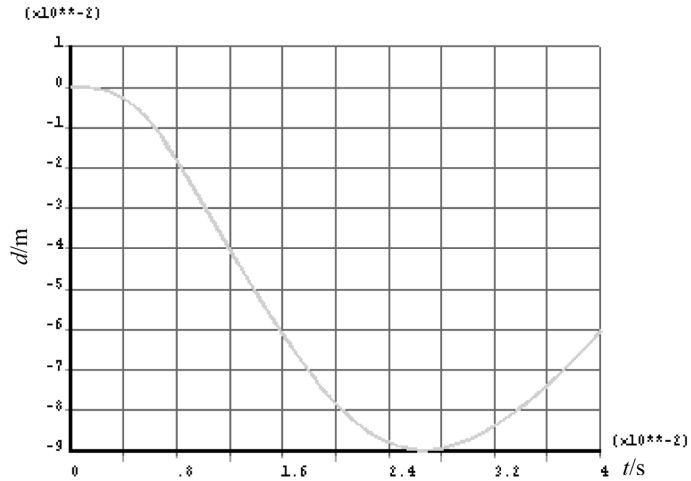


Fig. 15 The displacement ($d$) course with $K1$

Table 3 Simulating results with different spring stiffness

| Spring stiffness $K$ (N/m) | Max. $r2$ (N) | Max. $d$ (mm) | n |
|---|---|---|---|
| 160000 | 1325 | 90 | 0.1325 |
| 198997 | 1663 | 85.35 | 0.1663 |
| 240000 | 1812 | 82.11 | 0.1812 |

the groundsill and the displacement ($d$) of the down tie-in with different spring stiffness.

Table 3 shows that, reducing the spring stiffness, the shock absorption coefficient $n$ and the extremum of the disturbing force ($r2$) of the groundsill is reduced, but the max. displacement ($d$) of the shock absorber system increased. On the contrary, increasing the spring stiffness, the shock absorption coefficient $n$ and the extremum of the disturbing force ($r2$) of the groundsill is increased, the max. displacement ($d$) of the shock absorber system reduced, but it will go against the shock absorption if the spring stiffness is very rigid. On the other hand, the spring stiffness is too low to establish the detonating pressure of the hole fired gun. So there is an optimization design for the spring stiffness of the shock absorber system.

### 5.2 Simulating of the plastic material parameter

For Mooney-Revlinits plastic material model, the strain energy density function $W$ is decided by the two material parameters $A$, $B$ and the Poisson ratio $\nu$ (Vegter *et al*. 2003, Yin *et al.* 2002, Kevin 2004, Desalvo and Swanson 1994).

$$W(I_1, I_2, I_3) = A(I_1 - 3) + B(I_2 - 3) + C\left(\frac{1}{I_3^2} - 1\right) + D(I_3 - 1) \tag{29}$$

where, $C = \frac{1}{2}A + B$, $D = \frac{A(5\nu - 2) + B(11\nu - 5)}{2(1 - 2\nu)}$, and $I_1, I_2, I_3$ is the invariable part of the Cauchy-Green distortion tensor $C$,

$$\begin{aligned} I_1 &= \lambda_1^2 + \lambda_2^2 + \lambda_3^2 \\ I_2 &= \lambda_1^2\lambda_2^2 + \lambda_2^2\lambda_3^2 + \lambda_3^2\lambda_1^2 \\ I_3 &= \lambda_1^2\lambda_2^2\lambda_3^2 \end{aligned} \tag{30}$$

$\lambda_1, \lambda_2, \lambda_3$ is the principal protraction ratio. The Cauchy-Green distortion tensor $C$ is given by the distortion grads $F$ in Eq. (27).

For the simulation of the shock absorber system, the material parameter $A$, $B$ are given for $A1 = 0.7$ MPa, $B1 = 0.29$ MPa, $A2 = 0.7$ MPa, $B2 = 0.4$ MPa. The Poisson ratio is $\nu = 0.4997$. Fig. 16 and Fig. 17 show the simulating course of the disturbing force ($r2$) of the groundsill, plastic touching force ($r1$) with the down tie-in, plastic friction ($r3$) with the outer pipe and the displacement ($d$) of the down tie-in.

Table 4 shows the simulating shock absorption coefficient $n$ and the extremum of the disturbing force ($r2$) of the groundsill, plastic touching force $r1$ with the down tie-in, plastic friction ($r3$) with the outer pipe and the displacement ($d$) of the down tie-in with different plastic material parameters.

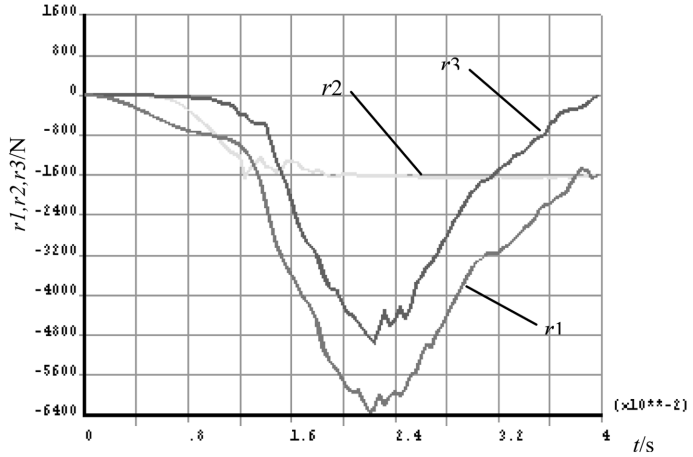


Fig. 16 The $r1$, $r2$ and $r3$ course with $A1$, $B1$

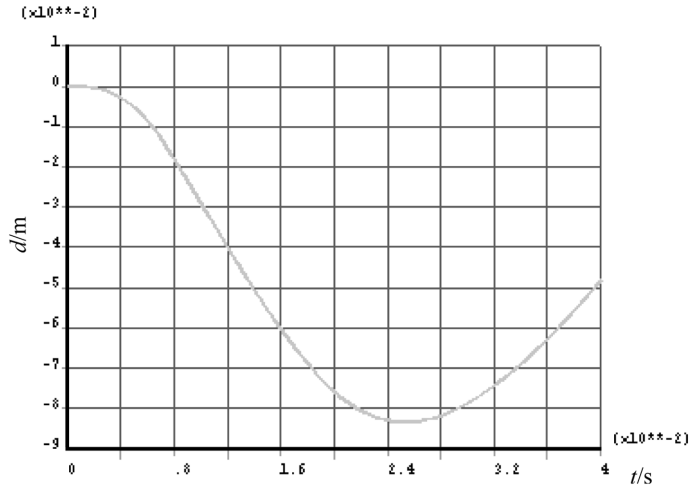


Fig. 17 The displacement ($d$) course with $A1$, $B1$

Table 4 Simulating results with different material parameter

| plastic parameter (MPa) | | Max. $r2$ (N) | Max. $d$ (mm) | $n$ | Max. $r3$ (N) | Max. $r1$ (N) |
|---|---|---|---|---|---|---|
| A | B | | | | | |
| 0.5 | 0.29 | 1663 | 85.35 | 0.166 | 5375 | 6647 |
| 0.7 | 0.29 | 1644 | 83.3 | 0.164 | 4940 | 6313 |
| 0.7 | 0.4 | 1999 | 82.1 | 0.199 | 5264 | 6891 |

Increasing the material parameter $A$, the plastic friction ($r3$) with the outer pipe reduced, but the extremum of the disturbing force ($r2$) of the groundsill and the amplitude changed little, the effect of the shock absorption can be ignored. Increasing the material parameter $B$, the extremum of the disturbing force ($r2$) of the groundsill and the plastic friction ($r3$) with the outer pipe increased, the

Table 5 Simulating results with different mass of the down tie-in

| mass of the down tie-in (kg) | Max. $r2$ (N) | Max. $d$ (mm) | $n$ |
|---|---|---|---|
| 7 | 1592 | 98 | 0.1592 |
| 11 | 1663 | 85.35 | 0.1663 |
| 15 | 1407 | 78.2 | 0.1407 |

effect of the shock absorption is debased.

### 5.3 Simulating of the mass of the down tie-in

Changing the mass of the down tie-in, Table 5 shows the simulating results of the shock absorber system with the different mass of the down tie-in. Reducing the mass of the down tie-in, the shock absorption coefficient $n$ reduced, but the amplitude of the shock absorption is increased, on the contrary, increasing the mass of the down tie-in, the shock absorption coefficient $n$ reduced, and the amplitude of the shock absorption is reduced too, so better effect of the shock absorption can be gained by increasing aptly the mass of the down tie-in.

## 6. Conclusions

Based on the finite element analysis simulating and experiment research, it is shown that the new designed shock absorber system has good capability of shock absorption for the impact load. Simulating shows that the effect of the shock absorber can be improved by reducing the material parameter $B$, or increasing aptly the mass of the down tie-in, the spring stiffness of the shock absorber system has an optimum design.

## References

Choi, S.B. and Hong, S.R. (2004), "Dynamic modeling and vibration control of electrorheological mounts", *J. Vib. Acous.*, **126**(4), 537-541.

Desalvo, G.J. and Swanson, J.A. (1994), ANSYS Engineering Analysis System-Theoretical Manual (V5.3), Houston Swanson Analysis, Inc.

Fortgang, J. and Singhose, W. (2002), "Concurrent design of input shaping and vibration absorbers", Presented at American Control Conference, Anchorage, Alaska.

Gao, W., Chen, J.J., Hu, T.B., etc. (2004), "Optimization of active vibration control for random intelligent truss structures under non-stationary random excitation", *Struct. Eng. Mech.*, **18**(2), 137-150.

Hartog, J.P.D. (1985), *Mechanical Vibrations*. New York: Dover Publications, Inc.

He, Z.H., Wu, W.Y., Chen, R.Q., etc. (2000), "A new model of damped vibration absorber", *J. China Text. Univ. (Eng. Ed.)*, **17**(3), 72-76.

Johan, M., Cronjé, P., Stephan Heyns, Nico, J. Theron, etc. (2004), "Development of a variable stiffness spring for adaptive vibration isolators", *Proc. of SPIE*, **5386**, 33-40.

John. O. Hallquist (1998), Ls-Dyna Theoretical Manual Livermore Software Technology Corporation.

Kevin K. Tseng (2004), "Modeling and simulation of porous lastoviscoplastic material", *J. Eng. Mech.*, **130**(5), 547-550.

Kim, J., King, Y.H., Choi, H.H. etc. (2002), "Comparison of implicit and explicit finite-element methods for the hydroforming process of an automobile lower arm", *Int. J. Adv. Manufacturing Tech.*, **20**, 407-413.
Pennestri, E. (1998), "An application of chebyshev's min-max criterion to the optimal design of a damped dynamic vibration absorber", *J. Sound Vib.*, **217**, 757-765.
Song, M.K., Noh, H.C., Kim, S.H., etc. (2005), "Control of free vibration with piezoelectric materials: Finite element modeling based on timoshenko beam theory", *Struct. Eng. Mech.*, **19**(5), 477-501.
The DYNAFORM Team, DYNAFORM User's Manual (V5.2), Engineering Technology Associates, Inc. 2004.
Vegter, H., Horn, C.H.L.J. ten, etc. (2003), "Characterisation and modeling of the plastic material behaviour and its application in sheet metalforming simulation", *Proc. 7th Int. Conf. on Computational Plasticity*. Barcelona.
Velichkovich, A.S. (2005), "Shock absorber for oil-well sucker-rod pumping unit", *Chem. Petroleum Eng.*, **41**(9), 545-546.
Yin, J.H., Zhu, J.G. and Graham, J. (2002), "A new elastic viscoplastic model for time-dependent behaviour of normal and overconsolidated clays: Theory and verification", *Can. Geotech. J.*, **39**, 157-173.